

SPECTRAL DENSITY OF STATES IN QUANTUM NANOCCLUSERS

Isa Kh. Zharekeshev

Al-Farabi Kazakh National University, Almaty

The density of states is studied by using disordered Hamiltonians for quantum systems. The electron spectrum of nanoclusters is calculated for various type of disorder.

The knowledge of the electron spectra in semiconductor structures of nanosizes is very important in modern condensed matter physics. This is related to the fact that due to quantum effects on the submicron scale the distance between the discrete neighbouring energy levels becomes less that the experimental temperature range, and less that the energy of inelastic scattering of electron-electron interaction. One of the powerful and constructive approaches for calculating the spectral density of states is direct modelling on the basis of Hamiltonians. In this paper we study the single-electron density of states of quantum systems in the presence of various types of impurity potential disorder.

We consider the spectrum of quantum particles in a random potential using the Anderson model. The Hamiltonian of the model on a simple cubic lattice is given by

$$H = \sum_{n\sigma} e_n c_{n\sigma}^+ c_{n\sigma} + \sum_{\langle n,m \rangle, \sigma} t_\phi (c_{n\sigma}^+ c_{m\sigma} + c_{n\sigma} c_{m\sigma}^+), \quad (1)$$

where $c_{n\sigma}^+$ creates an electron on the n -th site of a lattice. $\langle n,m \rangle$ implies that the second sum runs over those n and m which are nearest neighbours (the coordination number is $Z = 6$). The random potential is introduced via the on-site energies e_n (diagonal disorder). They are uniformly and independently distributed in the interval from $-W/2$ to $W/2$, i.e. according to the 'box' distribution.

$$P_B(W) = \frac{1}{W} \theta(|e_n - W/2|), \quad (2)$$

Here W denotes the strength of disorder. An Aharonov-Bohm flux ϕ is applied in all three directions (three-component flux). The transfer integral $t_\phi = t \exp(-2\pi i \phi a/L)$, contains a phase factor which is given by the flux in units of the flux quantum $\phi_0 = h/e$. In what follows we assume t and the lattice spacing a to be the units of energy and spatial distance, respectively. For $W = 0$ the Hamiltonian Eq.(1) corresponds to a conventional tight-binding model (TBM). The critical disorder at the band centre of this model is equal to $W_c = 16.5$ for $\phi = 0$. In addition to the 'box distribution', we probe another diagonal disorder, i.e. the model with the Gaussian distribution of the energies e_n :

$$P_G(W) = \frac{1}{\sqrt{\pi W^2/6}} \exp\left(-\frac{e_n^2}{W^2/6}\right), \quad (3)$$

The width of the Gaussian distribution is scaled in such a way that the second moments of $P_B(W)$ and $P_G(W)$ coincide: $\sigma_B(W) = \sigma_G(W) = W^2/12$. Correspondingly, at the band centre when $E = 0$ the critical disorder for this model $W_c = 20.9$ [1].

The Hamiltonian Eq.(1) is numerically diagonalized for simple cubic nanoclusters of different linear sizes L ranging from $L = 5$ to 32 . The computational procedure is based on the Lanczos algorithm for Hermitian matrices. First, we calculate the eigenvalues e_i with the precision less than 10^{-9} and construct histograms for the density of states $\rho(E)$ which is defined as follows:

$$\rho(E) = \frac{1}{L^3} \sum_n \delta(E - e_n), \quad (4)$$

here $\rho(E)$ is a global quantity, which is averaged of the whole volume of the nanocluster. Figures 1 and 2 demonstrate the spectral density of states $\rho(E)$ at various disorder W in the nanocluster of size $L=20$ with periodic boundary conditions for the uniform and the Gaussian distributions, respectively.

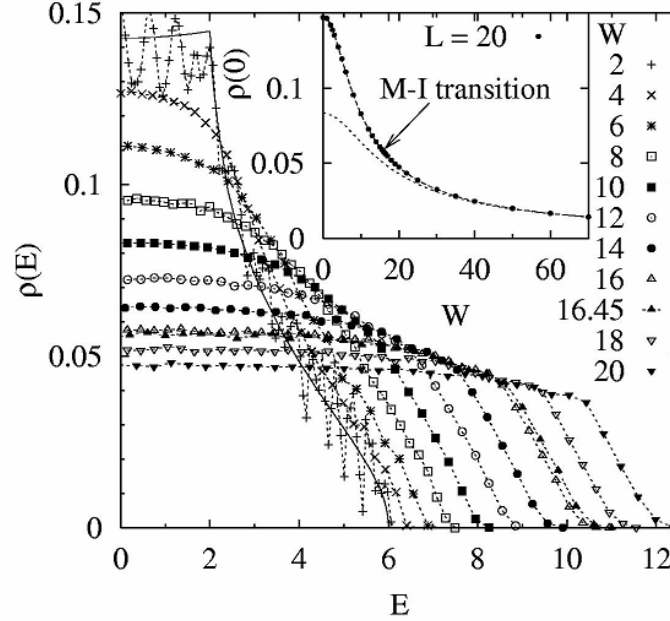


FIG. 1. The density of states $\rho(E)$ of the Anderson model for different strength of randomness W with the uniform distribution of the on-site energies Eq.(2). The data are obtained by direct diagonalization of a cubic quantum nanoclusters of linear size $L = 20$ for the Aharonov-Bohm flux $\varphi=0$ and averaged over many realizations. Solid line: result of the tight-binding model ($W=0$). Only the positive energy part is shown, due to symmetry with respect to the band centre $E=0$. Inset: The density of states at the band centre $\rho(0)$ as a function of disorder W . Solid line is the interpolation formula Eq.(5), dashed line is the Mott suggestion $\rho_M(0)$

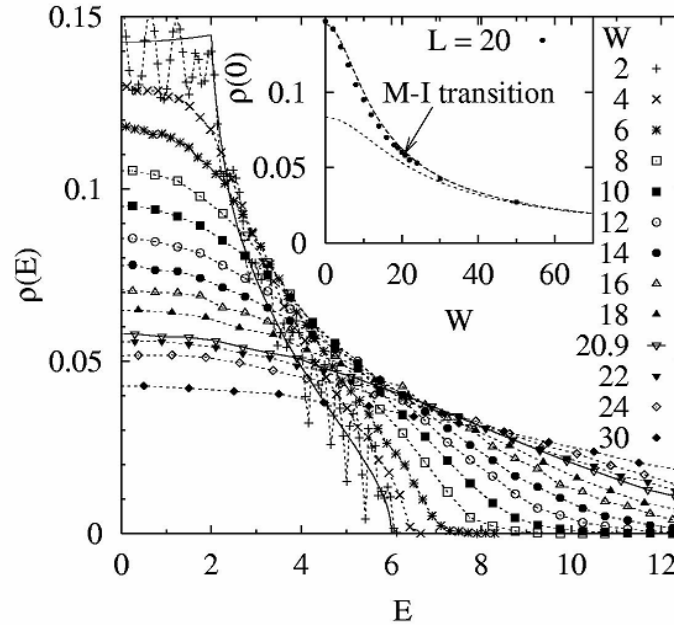


FIG. 2. The same as Fig. 1 for the Gaussian distribution of the on-site energies according to Eq.(3)

The oscillations of $\rho(E)$ for small disorder $W=2$ around the TBM result as one can observe in Fig.1 are due to finite size effects. At such a small disorder the mean free path is much larger than the system size $L = 20$. In fact, the spectrum of a clean ($W=0$) finite system consists of a

countable number of discrete highly degenerated levels, because the quasi-momentum operator commutes with the Hamiltonian. Clearly, the number of the energy levels, their degeneracy and positions depend on the size L , the lattice structure and the type of boundary conditions [2]. The TBM result is only applicable in the thermodynamic limit. In the case of small randomness the Brillouin zone is only slightly destroyed and the quasi-momentum is still a good quantum number. Due to non-zero disorder the degeneracy is lifted yielding a set of overlapping sub-bands. The shape of the density of states $\rho(E)$ is symmetric around the band centre $E = 0$, if the total number of the lattice sites L^3 is even or infinite.

With further increasing randomness W and the size L the overlap becomes stronger leading to smoother behaviour of $\rho(E)$. It is clear, that the forms of the density of states for sufficiently small W ($W < 2Z$) are almost equivalent for the both disorder models P_B and P_G . Close to the critical disorder $W_c = 16.5$ for the box distribution the density of states is nearly constant in a wide central part of the spectrum and is insensitive to the system size, provided that the size is sufficiently large. Compared to the Gaussian distribution, it starts to decay drastically with the energy E only in the vicinity of the band edges. This is due to a strict energy-range confinement of P_B , which allows for the exact bounds of the band edge, in contrast to P_G .

The typical energy range of this decay is of order of the hopping integral t and does not depend on disorder for $W > t$, while the band edge grows linearly with W . Obviously, in the limit of $W \gg 2Z$ the shape of $\rho(E)$ for both disorder models must tend towards the 'bare' distributions P_B and P_G , because the diagonal part of the Hamiltonian Eq.(1) dominates over the hopping elements. The disorder dependence of the density of states exactly at the band centre $\rho(E = 0)$ is shown in the inset of Fig. 1. It has been suggested by Mott [3], that $\rho(0)$ varies with increasing W according to $\rho_M(0) = (B^2 + W^2)^{-1/2}$, with $B = 2Z$ being the width of the unperturbed band. In fact, we have found that the numerical data are described better by the following interpolation expression:

$$P_G(W) = \frac{1}{\sqrt{\rho_{TBM}^{-2}(0) + P_B^{-2}(W)}}, \quad (5)$$

where $\rho_{TBM}(0) = 0.148$ and $P_B(W) = 1/W$ is simply the distribution of the on-site energies Eq.(2). We have checked for larger sizes $L > 20$ that the data fall onto the same curve irrespective to change of L . Notably, the equation (5) is of practical use for our unfolding procedure. The above interpolation works quite satisfactorily also for the Gaussian distribution (see inset of Fig. 2), the term P_B being substituted by $P_G(e=0)$. The results of our calculations for different non-zero values φ of the Aharonov-Bohm flux indicate that the averaged density of states is flux-invariant, although the positions of individual eigenvalues, as well as their short-range correlations depend on φ .

It should be noted that despite the present numerical data for the shape of $\rho(E)$ for various W are in reasonable agreement with the analytical results obtained within the coherent-phase approximation [4], a detailed comparative analysis is still required including also other types of diagonal randomness, e.g. the binary and the Lorentzian distributions of the on-site energies.

It is interesting to compare the density of states of the Anderson model with that of the random matrix theory (RMT). We have diagonalized the hermitian matrices whose all entries h_{ij} , with $i, j \leq N$ are distributed around zero according to the box distribution Eq.(2) with the variance $\sigma_B = 1/12$ (i.e. with $W = 1$). For both the orthogonal ($\beta = 1$) and the unitary ($\beta = 2$) matrices of size $N = 100$ the density of states $\rho(E)$ is averaged over 10000 random realizations (and for $N = 1000$ over 20 realizations). As shown in Fig. 3, the results for different N and for both types of symmetry are well described by the semicircle formula valid for the density of states of RMT (see also refs in book [5]) in the limit $N \gg 1$.

$$\rho_{RMT}(E) = \frac{1}{2\beta\pi N\sigma_b} \sqrt{4\beta N\sigma_b - E^2}, \quad (6)$$

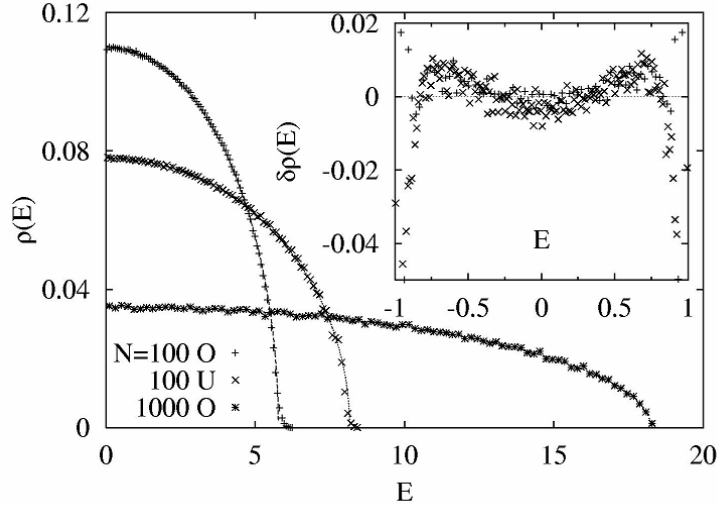


FIG. 3. The density of states $\rho(E)$ of the random matrices of different size $N \times N$ calculated numerically for the orthogonal ($N=100$ and 1000) and the unitary symmetry ($N = 100$) with the box distribution for all their elements Eq.(2) $W = 1$. Continuous lines are the semicircle density of states $\rho_{RMT}(E)$ Eq.(6). Only positive half of the band is shown because $\rho(E)$ is symmetric with respect to $E = 0$. Inset: relative deviations $\delta\rho(E)$ of the numerical results from $\rho_{RMT}(E)$ for $N = 100$ for orthogonal (+) and unitary (x) symmetry. Energy is rescaled according to $E \rightarrow E/(4\beta N\sigma_B)^{-1/2}$ (see text)

After rescaling $E \rightarrow E/(4\beta N\sigma_B)^{-1/2}$ the equation (6) becomes universal $\rho_{RMT}(E) = \sqrt{1 - E^2}$, irrespective to the size N and the symmetry β . One observes, however, the deviations from $\rho_{RMT}(E)$, particularly at the band edges, which diminish with increasing the size of the matrices N . The relative difference $\delta\rho(E) = \rho(E)/\rho_{RMT}(E) - 1$ between our finite- N results and the limiting expression is shown in the inset of Fig. 2 for the two types of symmetry. For example, the typical systematic discrepancy for $N = 100$ lies within 1-2% in the central 3/4-part of the spectrum. The relative deviation becomes stronger close to the band edges.

References

1. Bulka B., Schreiber M., Kramer B., Z. Phys. 1987, 66, 21-29.
2. Zharekeshev I. Kh., Kramer B., Scaling of level statistics at the disorder-induced metal-insulator transition // Phys. Rev. B, 1995, 51, 17239-17242
3. Mott N. F., Davis E.A. Electronic processes in non-crystalline materials, Clarendon Press, Oxford, 1971, 456p.
4. Krohas J. // Physica A, 1990, 167, 231-236.
5. Mehta M.L., Random Matrices, Academic Press, Boston, 1991, 523p.

КВАНТТЫҚ НАНОКЛАСТЕРЛАРДАҒЫ КҮЙЛЕРДІҢ СПЕКТРЛІК ТЫҒЫЗДЫҒЫ

И.Х. Жәрекешев

Кванттық жүйелерге арналған реттелмеген гамильтониандарды қолданып күйлердің тығыздығы зерттелінеді. Нанокластерлердің электрондық спектрі ретсіздіктің әртүрлі түрлеріне арналып есептелінеді.

СПЕКТРАЛЬНАЯ ПЛОТНОСТЬ СОСТОЯНИЙ В КВАНТОВЫХ НАНОКЛАСТЕРАХ

И.Х. Жәрекешев

Изучается плотность состояний с использованием неупорядоченных гамильтонианов для квантовых систем. Электронный спектр нанокластеров вычисляется для различных типов беспорядка.